Cent. Eur. J. Chem. • 10(1) • 2012 • 137-145
DOI: 10.2478/s11532-011-0129-0

VERSITA

Central European Journal of **Chemistry**

In vitro bioactivity of 70 wt.% SiO_2 - 30 wt.% CaO sol-gel glass, doped with 1, 3 and 5 wt.% NbF_5

Research Article

Lachezar Radev[1*], Katia Hristova[1], Valery Jordanov[1],
Maria Helena V. Fernandes[2], Isabel Margarida M. Salvado[2]

[1]*University of Chemical Technology and Metallurgy, 1756 Sofia, Bulgaria*

[2]*University of Aveiro, CICECO, 3810-193 Aveiro, Portugal*

Received 21 May 2011; Accepted 21 September 2011

Abstract: The $70SiO_2$-30CaO (wt.%) sol-gel glasses doped with 1, 3 and 5 NbF_5 (wt.%) were prepared *via* polystep sol-gel route. The synthesized glasses were characterized by XRD, FTIR and SEM. Changes in 1.5 SBF solutions were measured by ICP-AES. XRD of the glasses stabilized at 700°C for 6 hours proved the presence of niocalite. FTIR was consistent with XRD data. The *in vitro* bioactivity study of all glasses prepared were carried out by soaking in 1.5 simulated body fluid (1.5 SBF) at 37°C for 6 and 12 days in static conditions. The FTIR reveals the formation of A-type and B-type carbonate containing hydroxyapatite (CO_3HA) layer. Changes in 1.5 SBF solutions, after 6 days of soaking, show that the Ca concentration increased significantly, compared to the initial Ca content in the 1.5 SBF solution before *in vitro* test. After 12 days of immersion, the Ca concentration decreased, *i.e.*, the formation of HA phase consumed Ca from 1.5 SBF solution. For all soaking times, the concentration of P is much lower than that the used 1.5 SBF. Based on these results we suggest that Ca and P play an active role in the future of the glasses. SEM depicts that the different morphology of hydroxyapatite can be formed as a function of soaking time.

Keywords: *SiO_2-CaO-NbF_5 • Sol-gel glasses • Niocalite • In vitro bioactivity*

1. Introduction

It is well known that the prerequisite for an artificial material to bond to living bone is the formation of a layer of an apatite with similar structure and composition to those of the bone mineral on its surface [1-3]. Abe *et al*. reported that the bonelike apatite layers can be formed, on various kinds of materials *in vitro* by the following biomimetic process [4]. In this process, a substrate is first set in contact with the particles of sol-gel glasses in a simulated body fluid (SBF), with ion concentrations nearly equial to those of human plasma. The calcium ions realised from the glass particles increases the ionic activity product of the apatite in the surrounding SBF and silicate ions realised from the glass particles, attach to the surface of the substrat to induce apatite nucleation [5]. Other authors also have reported that the formation of silica gel layer on the surface, during the *in vitro* test, plays a fundamental role in the nucleation and crysttalysation of carbonate containing hydroxyapatite (CO_3HA). Some reports have also suggested that apatite formation on the surface of materials would be enhanced by the presence of Nb-OH groups [6-8].

During last years, several research groups have developed new types of glasses, which have been prepared and characterized in binary SiO_2-CaO [9-13], ternary CaO-SiO_2-P_2O_5 [12,14-17] and quaternary CaO-P_2O_5-SiO_2-MgO [18] systems. Ebisawa *et al.* concluded that F^- reduced the bioactivity of CaO-SiO_2 glasses, because they suppresed dissolution of the calcium ions into the SBF solution [19]. The results obtained with CaF_2-modified CaO-SiO_2 glass showed that the *in vitro* hydrohyapatite formation on this glass decreased in comparison with CaO-SiO_2 glass modified with Na_2O, MgO, B_2O_3 and P_2O_5 [19]. Fujii *et al*. also reported that the fluoride ions dissolved in

* *E-mail: radev@abv.bg*

to the SBF in the same manner as Ca^{2+} suppresed the apatite deposition on the sufrace of the glasses in the NaF-CaO-SiO_2 system [20]. The same effect was observed in a series of papers by substituting CaF_2 for Na_2O in Bioglass 45S5 [21,22] and CaF_2 for CaO [23]. However there is still not enough information in the literature about phase composition, structure and *in vitro* bioactivity of sol-gel 70S30C glass systems , doped with other fluoride compounds, *i.e.*, NbF_5.

The main purposes of the presented work are to obtain 70S30C sol-gel glass doped with 1, 3 and 5 wt.% NbF_5 and to assess their *in vitro* bioactivity for different periods of time in static conditions.

2. Experimental procedure

2.1. Preparation of the sol-gel glasses

Four sol-gel glasses with nominal compositions, shown in Table 1, were synthesized *via* polystep sol-gel method.

Tetraethoxysilane TEOS (purity >98%, Fluka), calcium nitrate tetrahydrate ($Ca(NO_3)_2$•$4H_2O$, Fluka) and Nb_2O_5 (Fluka) were used for their synthesis as silicon, calcium and niobium pentafluoride (NbF_5) sources, respectively.

The first step of the preparinig procedure was to prepare SiO_2 sol from TEOS. TEOS was stirred under mixed solvent of C_2H_5OH and H_2O with a small amount of HCl acid as a catalyst in a volume ratio TEOS:C_2H_5OH:H_2O:HCl=1:1:1:0.01. After recognizing transparent solution of above muxture in approxymately 1 hour the solution of $Ca(NO_3)_2$•$4H_2O$ was aded under intensively stirring for 2 hours. The second step was to prepare NbF_5 solution by dissolving of Nb_2O_5 in 18 M HF acid. Furthermore, a NbF_5 solution was added to SiO_2-calcium nitrate tetrahydrate mixture to prepare SiO_2-CaO-NbF_5 sol. Gelation of the obtained sols took place in 3 days at room temperature. The gels obtained were added for 3 days at 80°C and dried at 120°C for 2 days. The dried gels were grounded and sieved, taking the grains ranging in size from 32 to 63 μm. Fractions of 0.5 g of podwer were compacted at 50 MPa uniaxial pressure and 150 MPa of isostatic pressure to obtain disks (13 mm diameter and 2 mm in height). Then gel disks were sintered at 700°C for 6 hours in accordance with Martinez *et al*. [10].

2.2. *In vitro* test for bioactivity in 1.5 SBF

The assessment of *in vitro* bioactivity was carried out in 1.5 simulated body fluid (1.5 SBF), which gave a composition and ionic concentration 1.5 higher than human plasma. The 1.5 SBF was prepared by dissolving the following chemicals reagent in distilled water: NaCl (11.9925 g), KCl (0.3360 g), $CaCl_2$•$2H_2O$ (0.5520 g), $NaHCO_3$ (0.5295 g), K_2HPO_4•$3H_2O$ (0.3420 g), $MgCl_2$•$6H_2O$ (0.4575 g), Na_2SO_4 (0.1065 g), 2 M HCl (35. 493 g), $(CH_2OH)_3CNH_2$ (9.0075 g). The solution was kept at 37°C and pH was regulated to be between 7.3 and 7.4. A few drops of 0.5% sodium azide (NaN_3) was added to the 1.5 SBF solution to inhibit the growth of bacteria [24]. The *in vitro* tests were carried out in static conditions by soaking the disks in 40 mL of 1.5 SBF in polyethylene containers maintained at 37°C.

2.3. Characterization techniques

The synthesized sol-gel glasses were characterized by FTIR in a Nicolet Magna-IR spectrometer 550, by SEM in a Jeol 6400 microscope at 15 kV, and by XRD in a Bruker D8 Advance diffractometer with CuKα radiation and SolX detector. The XRD and SEM were carried out on the surface of the glass samples; the FTIR analysis was performed on ~1 mg of the material scraped from the glass surface with a metal blade, as described in [16]. At each time point (6 and 12 days), the samples were taken out from 1.5 SBF and the ion concentrations of Ca and P in the solutions were measured by inductively coupled plasma atomic emission spectroscopy (ICP-AES, IRIS 1000, Thermo Elemental, USA).

3. Results and discussion

3.1. X-ray diffraction analysis

XRD analysis of the prepared 70S30C sol-gel glass which was thermally treated at 700°C for 6 hours, doped with 1, 3 and 5 wt.% NbF_5 is given in Fig. 1.

After thermal treatment of the 70S30C sample at 700°C for 6 hours, no XRD peaks were observed (data are not shown here). In the XRD patterns one broadened peak ranging from 20° to 30° (2θ, degree) can be observed. D. Lukito *et al*. reported that this halo is clearly related to Si-O-Si network and also concluded that the presence of this halo indicates the amorphous nature of the bioactive glass [9]. When 70S30C sol-gel glasses were prepared in the presence of 1, 3 and 5 wt.% NbF_5, XRD detects the attendance of well-defined peaks of niocalite ($Nb_2Ca_{14}(Si_2O_7)_4O_8F_2$) based

Table 1. Chemical composition of the prepared sol-gel glasses.

N	Sample	Composition of the gel, wt.%		
		SiO_2	CaO	NbF_5
1	70S30C	71.5	28.6	-
2	70S30C1Nb	70.0	28.0	2.0
3	70S30C3Nb	67.3	26.9	5.9
4	70S30C5Nb	64.6	25.8	9.6

on the PDF 75-1704. It has been observed that the intensities of the niocalite peaks are gradually increasing. The niocalite lines are very sharp and more intense for the higher concentration of NbF_5.

3.2. FTIR of the prepared samples

3.2.1. FTIR of the samples before in vitro test in 1.5 SBF

FTIR spectra of the thermally treated glass samples (700°C for 6 hours) without or with NbF_5 in different weight ratio are given in Fig. 2.

As it is known, the higher frequency vibrations in the range 1034-1109 cm^{-1} corresponds to the v_{as}Si-O-Si bonds stretching vibrations [11,15,25]. In our case, when NbF_5 content increased in the prepared sol-gel glasses from 3 to 5 wt.%, the bands on the high energy site are strongly affected and new band located at 1109 (1110) cm^{-1} (Fig. 2, curves 3 and 4) is becoming dominant. The presence of these bands can be attributed to the vibration of [NbO_6] octahedra in accordance with Petit *et al*. [26] and Ayyub *et al*. [27] for the other systems in the presence of Nb^{5+}. According to other literature data, the band around 1110 cm^{-1} refers to the bridge oxygen of the S_2O_7 units. Its wavenumber as a function of the Si-O_b bond length adjusted to Si-O_b-Si bond angle of 133, fits well in the series of some sorosilicates, where O_b is the bringing oxygen [28,29].

The lower-frequency modes, observed in the 813-787 cm^{-1} region are due to the symmetric Si-O-Si stretching vibration [11,12,30-32]. The new bands appeared at 867-850 cm^{-1} (Fig. 2, curves 2-4) can be attributed to the presence of Nb-O bond in the highly distorted NbO_6 octahedra, as can be seen from Raman spectra, presented by others in different niobium containing glasses [33-35]. Makreski *et al*. found that the bands posited at 854-850 cm^{-1} could be assigned to the presence of v(Si-O_{nb}), where O_{nb} is the non bringing oxygen [28]. Bending modes of Si-O-Si and O-Si-O bonds are observed in 463-472 cm^{-1} region (Fig. 2, curves 1-4) in accordance with [11,12,14,15,25,28,36]. Consisitent with Heier and Poepelmeier's work, the bands centered at 470, 472 and 465 cm^{-1} for the NbF_5 doped 70S30C glass, may be attributed to vNb-F [37] or the bending mode of silicon-oxygen tetrahedron coordination, according to [31], for other sorosilicates.

For 70S30C sample (Fig. 2, curve 1) the band posited at 934 cm^{-1} may be assigned to the Si-O-Ca vibration mode [12,15], containing non bringing oxygen (NBO) [11]. On the other hand, M. Ziolek *et al*. described that the band centered at ~961 cm^{-1} in NbMCM-41 zeolites is due to a Si-O vibrational mode perturbed in the presence of different metal ions [38]. Others use this band for evidence the incorporation of metal ion in to the siliceous network (Si-O-T) [39-43]. From the obtained FTIR spectra depicted in Fig. 2 (curves 2-4) it can also be seen that when the quantity of NbF_5 increases in the 70S30C gel, the position of Si-O-Nb bond is shifted to higher values from 963 to ~973 cm^{-1}. From the preliminary investigations, the presence of those bands could be assigned to the formation of $NbOF_5^{2-}$ in the prepared samples [37].

At Fig. 2 FTIR spectra two additional bands can be observed: one at 656-643 cm^{-1} and other

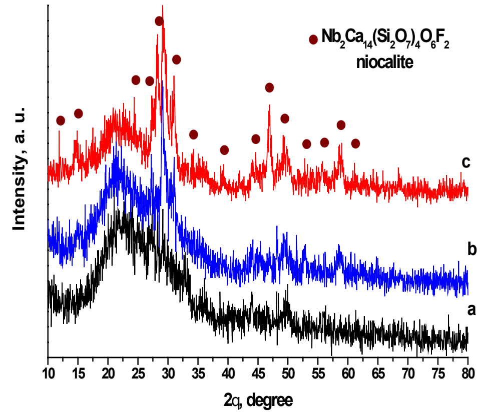

Figure 1. XRD patterns for 70S30C1Nb (a), 70S30C3Nb (b) and 70S30C5Nb (c) after annealing at 700°C for 6 hours.

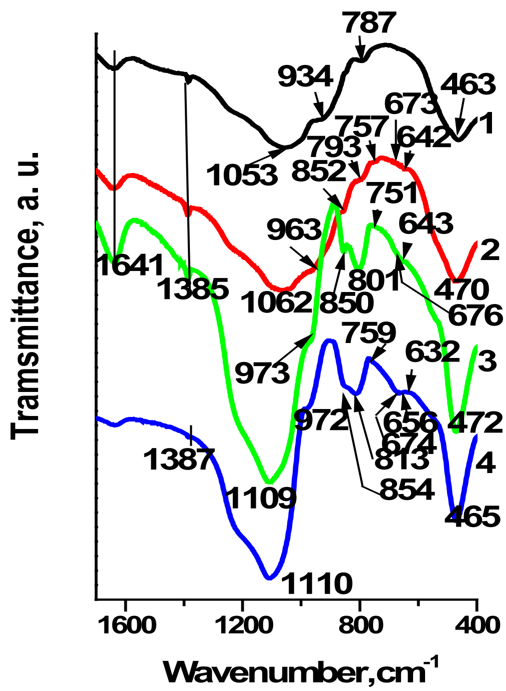

Figure 2. FTIR spectra of the obtained 70S30C (1), 70S30C1Nb (2), 70S30C3Nb (3) and 70S30C5Nb (4) sol-gel glasses after stabilization at 700°C for 6 hours in the region 1650-400 cm^{-1}.

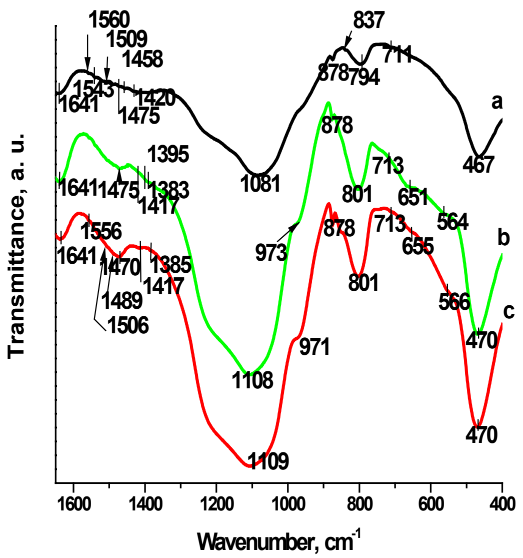

Figure 3. FTIR spectra of 70S30C1Nb (a), 70S30C3Nb (b) and 70S30C5Nb (c) after 6 days of immersion in 1.5 SBF in the region 1650-400 cm^{-1}.

at 759-742 cm^{-1}. The presence of these bands can be related to Nb-O bond in the synthesized samples [26,34,35,44-46]. For the glasses in BaO-MnO-SiO_2 system, I. Georgieva *et al*. found that the band centered at 656 cm^{-1} can be assigned to the presence of Si_2O_7 groups [31]. In addition, the ν_s(Si-O_b-Si) vibration localized on the bringing oxygen (O_b) between Si_2O_7 groups at 674 (676) cm^{-1} was different from that of the SiO_4 groups, as well as, the ν_{as}(Si-O_b-Si) vibration at ~1110 cm^{-1} [28,36,47].

As it can be seen for all samples (curves 1-4) the bands at 1383-1387 cm^{-1} and the band at 701 cm^{-1} for 70S30C1Nb sample (Fig. 2, curve 1) can be assigned to the presence of calcite and aragonite after annealing at 700°C for 6 hours [23,48,49]. In accordance with Martinez *et al*. [10] we can also observed the presence of absorption bands with slow intensity at 1434, 1461 and 1478 cm^{-1} for 70S30Ca sample (data are not shown in the spectrum, Fig. 2, curve 1). These bands can be ascribed to the presence of CO_3^{2-} groups [10]. In the samples doped with NbF_5 (Fig. 2, curves 2-4) the bands between 1430-1480 cm^{-1} are of very low intensity and corresponding to CO_3^{2-} groups. The presence of calcite and aragonite could be attributed to the process of replacement $Nb^{5+} \rightarrow Ca^{2+}$ in the SiO_2-CaO-xNbF_5, where x=1, 3 and 5 wt.% NbF_5. The vibration due to the OH bonds is observed for all samples (Fig. 2, curves 1-4) at 1641 and 1649 cm^{-1}. The intensity of this band decreases with increasing of NbF_5 content (Fig. 2, curves 2-4).

Briefly, from the obtained FTIR results we can conlude that :

• The addition of NbF_5 to 70S30C glass has a result of a shift from 1053 cm^{-1} to 1062 cm^{-1}, the appearance of a new active bands at 1109 (1110) cm^{-1} and ~675 cm^{-1}. In principle these bands could be related to the incorporation of niobium atoms in the glass network. Evidently, the increasing of the NbF_5 content to 3 wt.% results in the increase of the peak at 1109 cm^{-1}.

• The presence of Si-O-Nb bonds at 963, 973, 972 cm^{-1} could be assigned to the incorporation of Nb^{5+} in to silica matrix.

• The bands at 656, 674, 676 and ~1110 cm^{-1} could be ascribed to the Si_2O_7 groups, *i.e.*, FTIR confirmed XRD analysis.

• The bands posited at 701, 1383-1387 cm^{-1} can be assigned to the presence of calcite or aragonite. $CaCO_3$ content could be attributed to the replacement of Ca^{2+} from Nb^{5+}.

3.2.2. FTIR of the samples after in vitro test in 1.5 SBF for 6 and 12 days

Figs. 3 and 4 show the infrared spectra of the synthesized 70S30C sol-gel glasses doped with 1, 3 and 5 wt.% NbF_5 after *in vitro* test for 6 and 12 days in 1.5 SBF in the region 1650-400 cm^{-1}.

The IR spectrum of the immersed samples depicts the presence of broad peaks at around 1080-1110 cm^{-1}. These peaks are due to both the ν_1-ν_3 PO_4^{3-} and the most intense SiO_4^{4-} absorption band [50]. From the obtained results we can conclude that the ν_2 PO_4^{3-} signals are masked by another Si-O-Si vibration, and the only well-defined PO_4^{3-} band thus the doubly degenerate ν_4 PO_4^{3-} mode. On the other hand, the well-defined peaks at 794, 801 and 808 cm^{-1} are all attributed to the presence of Si-O-Si bonds in our sol-gel glasses doped with different quantity of NbF_5. In addition, the band at ~740 cm^{-1}, which can be attributed to the substitution of F^- by OH^-, is not distinguishable to the studied samples. The presence of OH^- groups is confirmed by the faint absorption bands, posited at ~3560-3570 cm^{-1} (not shown in Figs. 3 and 4).

The ν_1 mode of the PO_4^{3-} ion is represented in apatite by a very narrow band centered at 973 cm^{-1} [51] and the ν_3 mode produces an absorption peak posited at ~ 465-472 cm^{-1} for the doped with NbF_5 70S30C sol-gel glass [52-54]. Other authors proved that the bending modes of Si-O-Si and O-Si-O bonds are observed at 465-472 cm^{-1} [11]. On the other hand, as we have already written before, the bands in the region from 465 to 472 cm^{-1} may be attributed to the presence of νNb-F [37]. As it is shown by Rey *et al*., the main absorbance signal of PO_4^{3-} appears in the triply degenerate ν_3 domain [55]. Finally, the ν_4 modes gives two main bands posited at 651 cm^{-1} (Fig. 3, curve b) and

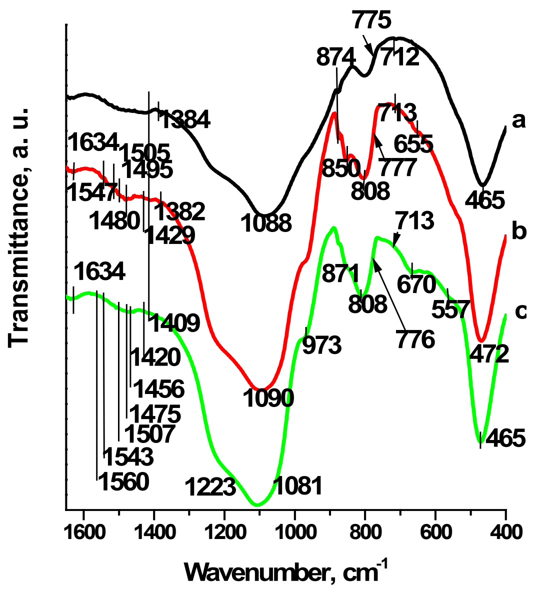

Figure 4. FTIR spectra of 70S30C1Nb (a), 70S30C3Nb (b) and 70S30C5Nb (c) after 12 days of immersion in 1.5 SBF in the region 1650-400 cm^{-1}.

653 (670) cm^{-1} (Fig. 4, curve b) and a shoulder at 564 (557) cm^{-1} (Fig. 3, curves b and c) and 557 cm^{-1} (Fig. 4, curves b and c) [52,53,56,57]. From the presented FTIR spectra, we can see that no additional bands are present in either the v_3 or v_4 domains, and, therefore, no distinguishable nonapatic environments or ions, *i.e.*, HPO_4^{2-}, are present in the precipitated mineral phase. In addition, the bands posited at 775, 777 and 776 cm^{-1} in all spectra presented in Fig. 4, curves a-c can be assigned to Nb-OH groups [58].

In earlier 1989, Rey *et al*. wrote that among the four internal vibrational modes of the free CO_3^{2-}, only two are of importance for infrared investigations in crystalline calcium phosphates: v_2 and v_3 [59]. The presence of the bands centered at 712 (713) cm^{-1} for the all samples, indicates that the $CaCO_3$ is associated with our samples after *in vitro* test in 1.5 SBF for 6 and 12 days of soaking. Ivankovich and his co-workers proved that these bands can be assigned to the presence of aragonite on the immersed samples [60]. Lusvardi and co-authors proved that $CaCO_3$ was monitored by the presence of the peak posited at ~715 cm^{-1} [23]. They also concluded that the precipitation of calcium carbonate is a specific property of CaF_2-modified 45S5 sol-gel glasses [23]. H. Feki *et al*. proved that in fluorinated apatites, the bands posited at ~718 cm^{-1} could be ascribed to the presence of B-type CO_3HA [61]. In addition the peak at 850 cm^{-1}, for the 70S30C3Nb sample (Fig. 4, curve b), was also assigned to the presence of small amounts of aragonite, according to [60]. The v_3 mode at 1400-1560 cm^{-1} for all samples, corresponding to the strongest infrared peaks of the CO_3^{2-} is composed by three bonds. In the series of papers the v_3 CO_3^{2-} peaks in CO_3HA at 1397 (1409) cm^{-1}, 1382, 1383, 1384 and 1389 cm^{-1}, and 1417, 1420 and 1429 cm^{-1} were observed [52-54,57,60].

The infrared spectrum of the CO_3^{2-} ion in apatite has been explained by the presence of CO_3^{2-} in two environments, as presented in [62]. It is now widely accepted that CO_3^{2-} substitutes either for the column ions OH^- and F^- or for PO_4^{3-} in the apatite structure. Regnier and his colleagues wrote that this substitution into different crystallographic sites results in two sets of absorption bands corresponding to A-type CO_3HA substitution (1540-1460-878 cm^{-1}) and B-type CO_3HA substitution (1455-1420-871 cm^{-1}) [63].

In our case, the characteristic absorptions at 1540, 1543 and 1547 cm^{-1} are present in the spectrum of all samples, as it can be seen from Fig. 3 and Fig. 4 [52]. Furthermore, the absorption band at 1470-1475 cm^{-1} (Fig. 3 and Fig. 4, curve c) [56] and these at 878 cm^{-1} (Fig. 3 and Fig. 4) are also present [53,54,57,64]. They are also indicative for A-type CO_3HA on the prepared samples. In addition, the v_3 mode of B-type CO_3HA is clearly exhibited by the presence of 1455-1458 cm^{-1} [52-54,60,65], 1417-1420 cm^{-1} [54,64,66], 1382 cm^{-1} [67,68] and 871 (874) cm^{-1} [63] in to the synthesized samples after *in vitro* assay. v_3 bands at 1473-1475 cm^{-1} could be ascribed to the presence of B-type CO_3HA [62,69].

Another interesting feature in Figs. 3 and 4 is the slight displacement of the v_2 peak position toward lower wavenumbers from 878 cm^{-1} (for 3 and 5 wt.% NbF_5 after 6 days of immersion, Fig. 3 curves b and c) to 874-871 cm^{-1} (for the same samples after 12 days of soaking, Fig. 4) [64,66]. Based on the preliminary results, we can assume that this displacement is a function of fluoridization of the 70S30C sol-gel glass [63].

On the base of FTIR resuts we can conclude that:

• The prepared samples are *in vitro* bioactive. The inclusion of NbF_5 in to the gel with nominal composition 70wt.% SiO_2-30 wt.% CaO leads to the increasing of the *in vitro* bioactivity of the investigated samples.

• The nucleation of A-type and B-type CO_3HA were estimated on the obtained glasses after 6 and 12 days of soaking in 1.5 SBF.

3.3. Changes in 1.5 SBF solution

Fig. 5 concisely presents the evaluation of ionic concentration for Ca in the liquid over increasing time of immersion for 70S30C (sample 1) and for doped

70S30C with different weight% of NbF_5 (samples 2, 3 and 4) in 1.5 SBF at 37ºC for 6 and 12 days.

From Fig. 5 it can be seen that the concentration of Ca in 1.5 SBF solutions after 6 and 12 days for all samples, were monitored. When the quantity of NbF_5 in 70S30C sol-gel glass increased to 3 wt.%, the Ca concentration was significantly increased from 86 mg/l, which is the concentration of Ca in 1.5 SBF solution before *in vitro* test, to 849 mg L^{-1} for sample 3. With increasing of NbF_5 content (wt.%) in 70S30C sol-gel glass, the Ca concentration was decreased to 541 mg L^{-1}, respectively. After 12 days of soaking of the studied samples in 1.5 SBF, the Ca concentration slightly decreased with the increasing of NbF_5 content in 70S30C sol-gel glass (samples 3 and 4). Nevertheless, in the crystalline calcium phosphates formation there are included already formed Nb-OH in accordance with FTIR observations (Fig. 4) [58,70]. From the others preliminary results [9], we can conclude that there are two processes of mass-transfer in the soaking procedure: (1) ion exchange of Ca ions in pure 70S30C sol-gel glass and in doped with different quantity of NbF_5 gel glass, which would increase the Ca concentration in the 1,5 SBF solution, and (2) the formation of hydroxyapatite phase on the surfaces of the immersed samples, doped and not doped with NbF_5, which would consume Ca and give a decrease of Ca concentration in 1.5 SBF solution. Furthermore, for all soaking times, the concentration of P (mg L^{-1}) in 1.5 SBF solutions were less than 1 mg/l, which is much lower than that of the 1.5 SBF (68 mg L^{-1}) used. This fact demonstrates that the PO_4^{3-} ions in 1.5 SBF solutions were consumed by the formation of hydroxyapatite layer [9]. Agathopoulos *et al*. observed that in the case of CaO-MgO-SiO_2 modified with B_2O_3, Na_2O, CaF_2 and P_2O_5, after immersion in SBF from 1 to 42 days, phosphorus concentration was rapidly decreased. On the base of these results, the authors suggests that P may play an active role on the transformation of glass surface during the immersion in SBF for long periods of time [71].

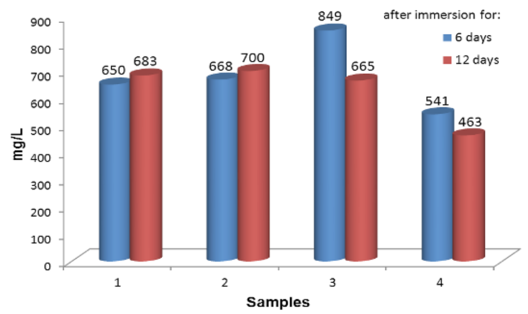

Figure 5. Changes in calcium content from the 70S30C (sample 1), 70S30C1Nb (sample 2), 70S30C3Nb (sample 3) and 70S30C5Nb (sample 4) after *in vitro* test in 1.5 SBF for 6 and 12 days.

3.4. SEM observations after in vitro exposure in 1.5 SBF

SEM images of 70S30C sol-gel glass, doped with different quantity of NbF_5, after *in vitro* test, are given in Figs. 6 and 7.

The presented SEM images of the samples after 6 days of immersion in static conditions (Fig. 6a-6c) shows the presence of relatively dense microstructure

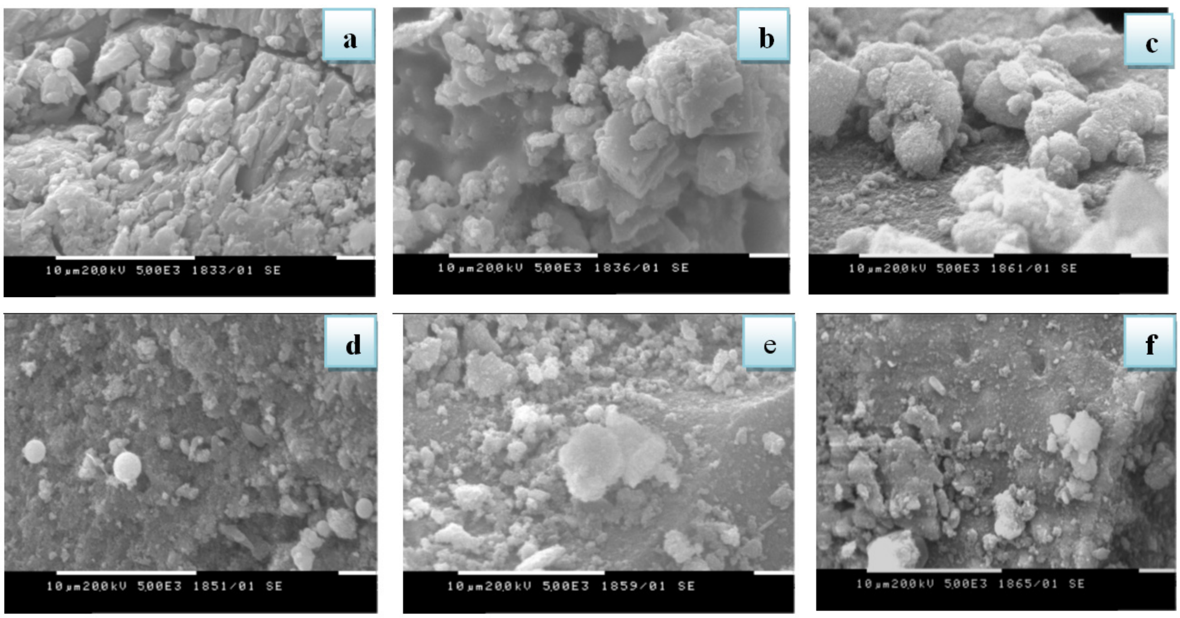

Figure 6. SEM images for the prepared samples after *in vitro* test in 1.5 SBF for 6 (a-c) and 12 (d-f) days: 70S30C1Nb (a, d), 70S30C3Nb (b, e) and 70S30C5Nb (c, f).

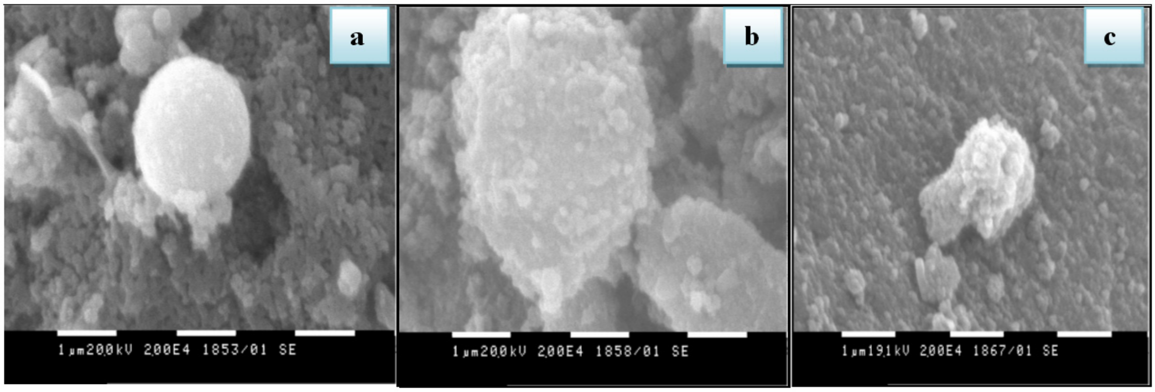

Figure 7. SEM images for the 70S30C1Nb (a) and 70S30C3Nb (b) and 70S30C5Nb (c) samples after 12 days of immesion in 1.5 SBF at high magnidication.

with different morphology: spheres with diameters from 0.6 to 1.6 μm and aggregated structures. On the basis of the obtained FTIR data (Fig. 3) and SEM images (Fig. 6), it could be concluded that hydroxyapatite phase was formed on the surface of the soaked samples. When the glasses were immersed for 12 days in 1.5 SBF, SEM images showed that spherical and aggregated particles are also deposited on the surface (Fig. 6d-6f). The diameters of the spheres were 1.3-2.2 μm. From the SEM images of the immersed for 12 days samples (Fig. 7a-7c), it may seem to us that the spheres and aggregated particles had crackles on their bumpy surface. But it is not. As it can be seen, the big particles are composed of small nanospheres. The diameter of these spheres reaches up to 0.2 μm.

4. Conclusions

All gel glasses with or without 1, 3 and 5 wt.% NbF_5 in the 70S30C system have been synthesized *via* sol-gel route. The structure of the prepared glasses were monitored with XRD, FTIR and SEM. The main conclusions were listed as follows:

1. After stabilization of the synthesized glasses, X-ray diffraction proved the presence of niocalite. The crystallinity of the niocalite phase increased with increasing of NbF_5 content. FTIR depicts that the niobium was incorporated into glass network.

2. The estimation of the *in vitro* bioactivity in 1.5 SBF demonstrates that all of the samples are *in vitro* bioactive. FTIR proved that the CO_3HA can be formed on the surface of the prepared glasses. CO_3HA consisted of both A- and B-type CO_3^{2-} ions. SEM micrograph depicted different forms of HA particles, precipitated on the surface, after immersion in 1.5 SBF for 6 and 12 days. After 12 days of soaking SEM images depicts the presence of some spherical particles, consisted of the small spheres with diameter of ~0.2 μm. Finally, NbF_5 has a positive effect on the *in vitro* bioactivity of 70S30C sol-gel glass.

3. Changes in 1.5 SBF solution, after 6 days of soaking, show that the Ca concentration was significantly incresed, compared to the initial Ca content in the 1.5 SBF solution before *in vitro* test. After 12 days of immersion, the Ca concentration decreased, *i.e.*, the formation of HA phase consume Ca from 1.5 SBF solution. For all soaking times, the concentration of P is much lower than that the used in 1.5 SBF. On the base of these results we suggest that Ca and P play an active role in the future of the glasses.

Acknowledgements

The authors kindly acknowledge the Chemistry Department at the University of Aveiro and the AQUACHIM JSC - Bulgaria for their support.

References

[1] T. Kokubo, J. Ceram. Soc. Jpn. 99, 965 (1991)
[2] T. Kokubo, Journal of Non-Crystalline Solids 120, 138 (1990)
[3] T. Kokubo, Biomaterials 12, 155 (1991)
[4] Y. Abe, T. Kokubo, T. Yamamuro, J. Mater. Sci.: Mater. Med. 1, 233 (1990)
[5] K. Hata, N. Ozawa, T. Kokubo, T. Nakamura, J. Ceram. Soc. Jpn. 109(5), 461 (2001)
[6] G. Ramirez, *et al*., Appl. Surf. Sci. 25, 2555 (2011)
[7] S. Nagarajan, V. Raman, N. Rajendran, Materials Chemistry and Physics 119, 363 (2010)
[8] A. Sugino, *et al*., Acta Biomaterialia 5, 298 (2009)
[9] D. Lukito, J.M. Xue, J. Wang, Materials Letters 59, 3267 (2005)

[10] A. Martínez, I. Izquierdo-Barba, M. Vallet-Regí, Chem. Mater. 12(10), 3080 (2000)

[11] G.S. Pappas, *et al*., Journal of Non-Crystalline Solids 354(2-9), 755 (2008)

[12] J. Roman, S. Padilla, M. Vallet-Regi, Chem. Mater. 15, 798 (2003)

[13] M. Vallet-Regi, *et al*., Solid State Ionics 172, 441 (2004)

[14] A. Ramila, F. Balas, M. Vallet-Regi, Chem. Mater. 14, 542 (2002)

[15] D. Arcos, D.C. Greenspan, M. Vallet-Regi, Chem. Mater. 14, 1515 (2002)

[16] M. Vallet-Regi, A. Ramila, Chem. Mater. 12, 961 (2000)

[17] M. Vallet-Regi, *et al*., J. Mater. Chem. 15, 1353 (2005)

[18] J. Perez-Pariente, F. Balas, M. Vallet-Regi, Chem. Mater. 12, 750 (2000)

[19] Y. Ebisawa, T. Kokubo, K. Ohura, T. Yamamuro, J. Mater. Sci.: Mater. Med. 1, 239 (1990)

[20] E. Fujii, *et al*., J. Ceram. Soc. Jpn. 111(10), 762 (2003)

[21] G. Lusvardi, *et al*., J. Phys. Chem. B 112(40), 12730 (2008)

[22] G. Lusvardi, *et al*., J. Phys. Chem. B 113(30), 10331 (2009)

[23] G. Lusvardi, *et al*., Acta Biomaterialia 5, 3548 (2009)

[24] G. Falini, S. Fermani, B. Palazzo, N. Roveri, J. Biomed. Mater. Res. A. 87(2), 470 (2008)

[25] N.J. Coleman, M. Bellantone, J.W. Nicholson, A.P. Mendham, Ceramics-Silikáty 51(1), 1 (2007)

[26] L. Petit, *et al*., Journal of Non-Crystalline Solids 351, 2076 (2005)

[27] P. Ayyub, M.S. Multani, V.R. Palkar, R. Vijayaraghavan, Phys. Rev. B 34(11), 8137 (1986)

[28] P. Makreski, *et al*., Vibrational Spectroscopy 44, 162 (2007)

[29] A. Cruz-Ramirez, *et al*., Journal of Fluorine Chemistry 132, 323 (2011)

[30] J. Garcıa, *et al*., Journal of Non-Crystalline Solids 354, 729 (2008)

[31] I. Georgieva, *et al*., J. Mater. Sci. 31, 3197 (1996)

[32] I. Georgieva - Mihailova, PhD Thesis (University of Chemical Technology and Metallurgy, Sofia, 1997)

[33] A.A. Lipovskii, *et al*., Journal of Non-Crystalline Solids 354, 1245 (2008)

[34] A. Flambard, *et al*., Journal of Non-Crystalline Solids 354, 3540 (2008)

[35] L.F. Santos, L. Wondraczek, J. Deubener, R.M. Almeida, Journal of Non-Crystalline Solids 353, 1875 (2007)

[36] Z. Yin, *et al*., Hydrometallurgy 103, 215 (2010)

[37] K.R. Heier, K.R. Poeppelmeier, J. Solid State Chem. 133, 576 (1997)

[38] M. Ziolek, *et al*., Catalysis Today 70, 169 (2001)

[39] J. Sarkany, J. Mol. Struct. 410-411, 95 (1997)

[40] J. Sarkany, J. Mol. Struct. 410-411, 137 (1997)

[41] J. Sarkany, J. Mol. Struct. 410-411, 145 (1997)

[42] Z. Sobalik, Z. Tvaruzkova, B. Wichterlova, J. Phys. Chem. B 102, 1077 (1998)

[43] E. Broclawik, J. Datka, B. Gil, P. Kozyra, Phys. Chem. Chem. Phys. 2, 401 (2000)

[44] R.F. Brandão, *et al*., J. Braz. Chem. Soc. 20(5), 954 (2009)

[45] I.O. Mazali, L.C. Barbosa, O.L. Alves, J. Mater. Sci.:Mater. Med. 39, 1987 (2004)

[46] D. Prasetyoko, Z. Ramli, S. Endud, H. Nur, Advances in Materials Science and Engineering 2008, 1 (2008)

[47] Z. Ding, Zh. Yin, H. Hu, Q. Chen, Thermochimica Acta 511, 168 (2010)

[48] A. Olad, A. Rashidzadeh, Iranian Journal of Chemical Enineering 5(2), 45 (2008)

[49] H. Tang, J. Yu, X. Zhao, D.H.L. Ng, Cryst. Res. Technol. 43(5), 473 (2008)

[50] L. Radev, *et al*., Processing and Application of Ceramics 4(1), 15 (2010)

[51] N. Pleshko, A. Boskey, R. Mendelsohn, Biophys. J. 60, 786 (1991)

[52] M. Markovic, B. Fowler, M.S. Tung, J. Res. Natl. Inst. Stand. Technol. 109, 553 (2004)

[53] V. Jokanovic, *et al*., J. Mater. Sci.: Mater. Med. 17, 539 (2006)

[54] I. Rehman, W. Bonfield, J. Mater. Sci.: Mater. Med. 8, 1 (1997)

[55] C. Rey, M. Shimuzu, B. Collins, M.J. Glimcher, Calcif Tissue Int. 49, 383 (1991)

[56] S. Koutsopoulos, J. Biomed. Mater. Res. 62, 600 (2002)

[57] I. Hofmann, L. Muller, P. Greil, F. Muller, J. Am. Ceram. Soc. 90(3), 821 (2007)

[58] O.C. Compton, F.E. Osterloh, J. Phys. Chem. C 113, 479 (2009)

[59] C. Rey, *et al*., Calcif. Tiss. Int. 45 157 (1989)

[60] H. Ivankovic, *et al*., J. Mater. Sci.: Mater. Med. 20, 1039 (2009)

[61] H. Feki, Ch. Ren, M. Vignoles, Calcif. Tissue Int. 49, 269 (1991)

[62] M. Fleet, X. Liu, P. King, American Mineralogist 89, 1422 (2004)

[63] P. Regnier, *et al*., American Mineralogost 79, 809 (1994)

[64] E. Landi, G. Geloti, G. Logrocino, A. Tampieri,

J. Eur. Ceram. Soc. 23, 2931 (2003)
[65] N. Hijon, M. Cabanas, I. Izquierdo-Barba, M. Vallet-Regi, Chem. Mater. 16, 1451 (2004)
[66] J. Lafon, E. Champion, D. Bernache-Assolant, J. Eur. Ceram. Soc. 28, 139 (2008)
[67] Y.-P. Guo, *et al*., Materials Letters, doi:10.1016/j.matlet.2011.04.057 (2011)
[68] M. Fleet, X. Liu, Biomaterials 28, 916 (2007)
[69] I. Khairoun, *et al*., J. Biomed. Mater. Res. 60(4), 633 (2002)
[70] T. Miyazaki, *et al*., J. Ceram. Soc. Jpn. 109(11), 929 (2001)
[71] S. Agathopoulos, *et al*., Biomaterials 27, 1832 (2006)